PRODUCTION OF HEAVY QUARKS AT HERA

Beate Naroska
Institut f. Experimentalphysik, Universität Hamburg
Luruper Chaussee 149, 22761 Hamburg
E-mail: naroska@mail.desy.de

A brief introduction to the status of heavy flavour production at HERA is given. The large data sample now available allows the production of open charm and beauty hadrons and of charmonium to be studied in detail. Comparisons of differential cross sections with NLO QCD calculations and Monte Carlo models are performed in photoproduction and in deep inelastic scattering. In the case of Charmonium a comparison with NRQCD predictions is also made.

1 Introduction

The production of charm and beauty quarks in ep, $\gamma\, p$, $p\bar{p}$ and $\gamma\gamma$ collisions is a testing ground for QCD. Broad agreement of perturbative QCD (pQCD) calculations with data has been established for the production of charm quarks, although some discrepancies exist in particular regions of phase space. The production of beauty quarks is not yet understood so well. Initially large deviations were found between the predictions of pQCD at next-to-leading order (NLO) and the measured b production rates.

At HERA, the main production process of c and b quarks is boson gluon fusion (BGF, figure 1a). Presently detailed investigations are being carried out in photopro-

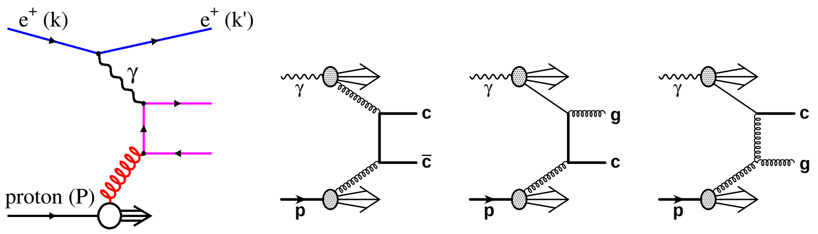

Figure 1: *Processes for direct (a) and resolved heavy quark production (b-d).*

duction, $Q^2 \rightarrow 0$, where the hadronic or resolved component of the photon plays a large role (e.g. figures 1b-d), and in deep inelastic scattering (DIS), $Q^2 \gtrsim 2$ GeV^2.

New opportunities arise, when the $c\bar{c}$ system hadronises into a J/ψ. This will be addressed in section 4.

2 Theoretical Considerations

The theoretical calculations which are used for comparison with the data on open heavy flavour production can be classified into two categories: calculations in pQCD and LO Monte Carlo Models in which higher orders are approximated by parton showers (LO+PS).

In the kinematic region $p_T^2 \lesssim m_{c,b}^2$, it is expected that NLO ($\mathcal{O}(\alpha_S^2)$) QCD calculations in the so-called massive scheme [1,2] will give reliable results. In this scheme, u, d and s are the only active quark flavours in the proton and heavy quarks are dynamically produced via BGF. In contrast, in the massless scheme, valid for $p_T^2 \geq m_{c,b}^2$, the heavy quarks are treated as sea quarks in the proton and in the resolved photon. Charm (or beauty) quarks can then directly emerge from within the photon (fig.1c-d) or proton.

Recently a 'matched' scheme was proposed [3], using a fixed order massive ansatz at low p_T^2 and a massless calculation at higher values, carefully avoiding double counting ('FONLL', fixed order + next to leading log).

The Monte Carlo models which are used for comparison with the data (mainly PYTHIA [4], HERWIG [5], RAPGAP [6] and CASCADE [7]) differ in many details. The majority use DGLAP evolution of parton densities, while CASCADE [7] implements CCFM evolution and off-shell matrix elements.

3 Charm Production

DIS New preliminary $D^{*\pm}$ cross sections were presented by the H1 collaboration for $Q^2 > 2$ GeV^2 [9] and $Q^2 \rightarrow 0$ [8]. For $Q^2 > 2$ GeV^2, the data from 1999/2000 were used [1], corresponding to 47 pb^{-1}. The inclusive cross sections in figure 2 are compared to NLO fixed order calculations and to the Monte Carlo models RAPGAP [6] and CASCADE [7]. The agreement of the NLO calculation is good within

[1]Kinematic region: $Q^2 > 2$ GeV^2; $0.05 < y < 0.7$, $p_T^{D^*} > 1.5$ GeV; $|\eta^{D^*}| < 1.5$.

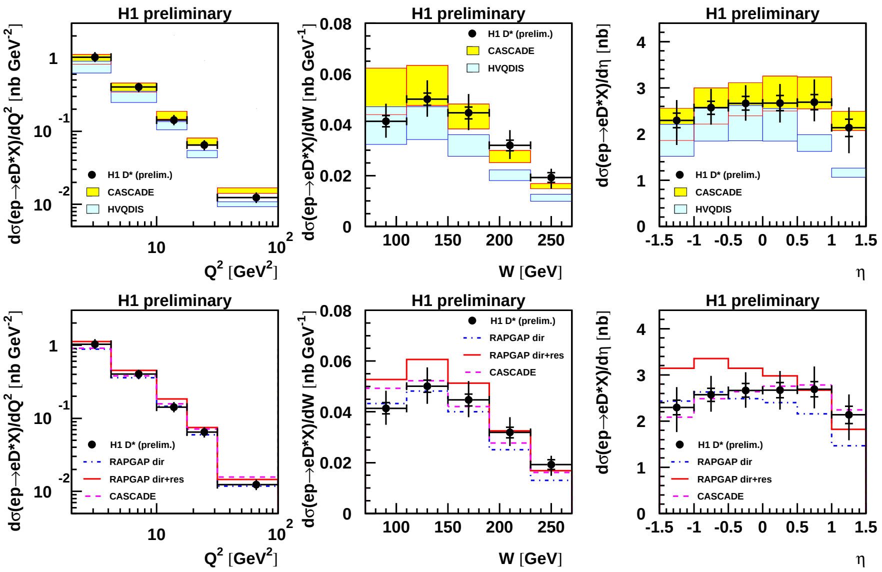

Figure 2: *Single differential inclusive cross section $\sigma(ep \to eD^{*\pm}X)$ versus Q^2, W and η_{D^*}. Top row: Data with the NLO DGLAP calculation (HVQDIS with CTEQ5F3 parton densities and hadronisation corrections, lower shaded band). The upper shaded band shows the CASCADE expectation. Bottom row: Comparison with RAPGAP Monte Carlo using the CTEQ5L parton densities and again CASCADE.*

errors and with CASCADE it is even better. Note that CASCADE describes the measurements at high η values. The LO + PS Monte Carlo calculation RAPGAP does not give as good a description of the data as the NLO calculations and CASCADE.

Demanding at least 2 jets[2] in addition to the D^* leads to a systematic deviation of both MC models from the data, shown in figures 3 and 4.

Photoproduction The new preliminary photoproduction analysis of H1 uses 49 pb^{-1} and is compared to preliminary ZEUS data [10] in figure 5. The kinematic regions [3] are slightly different. Both data sets show the same features in comparison to the NLO calculation: the theoretical curve falls below the data at positive η^{D^*} and

[2] $p_T^{jet} > 4(3)$ GeV; $-1 < \eta_{lab}^{jet} < 2$.

[3] H1 region, $Q^2 < 0.01$ GeV^2, $171 < W < 256$ GeV, $p_T(D^*) > 2.5$ GeV, $|\eta(D^*)| < 1.5$; ZEUS region, $Q^2 < 1$ GeV^2, $130 < W < 285$ GeV, $1.9 < p_T(D^{*\pm}) < 20$ GeV, $|\eta(D^{*\pm})| < 1.6$.

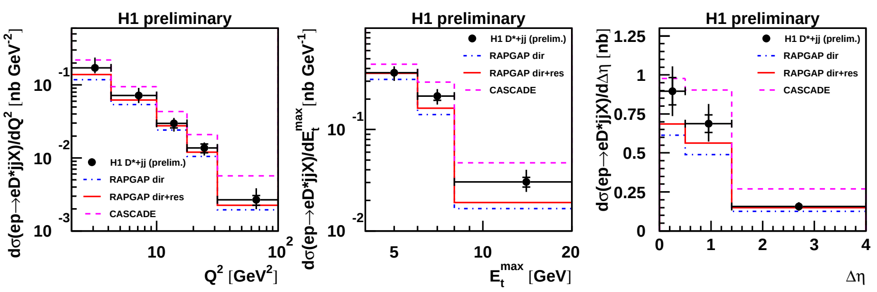

Figure 3: *Dijet cross sections as a function of Q^2, E_t^{max} and $\Delta\eta$ for events with $D^{*\pm}$ mesons. The expectation of the RAPGAP Monte Carlo (with $m_c = 1.4$ GeV, $\epsilon_c = 0.078$ and using the CTEQ5L parton densities in the proton) is shown with and without resolved contributions. The data are also compared with the expectation of the CASCADE Monte Carlo model.*

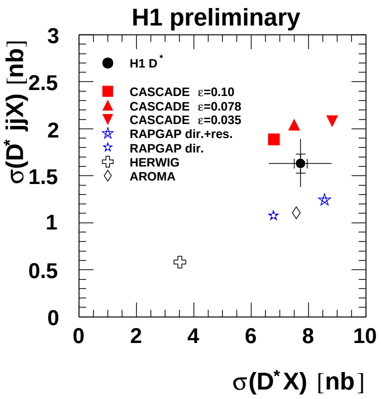

Figure 4: *The cross section for dijet production in events with a $D^{*\pm}$ meson versus the $D^{*\pm}$ meson production cross section is shown. The expectations of the RAPGAP, AROMA, HERWIG and CASCADE Monte Carlo models are also shown.*

at low $p_T^{D^*}$. These slight discrepancies are more pronounced in the H1 data set.

The "matched" FONLL calculation, which is shown with the ZEUS data, is not better than the NLO result and is below the data at high $p_T^{D^*}$. In contrast, the $p_T^{D^*}$ spectrum of CASCADE is found to be too hard in comparison to the H1 data.

3.1 Fragmentation

The non-perturbative input parameters necessary to model the hadronisation of charm quarks have been determined in e^+e^- collisions. The ZEUS collaboration has recently

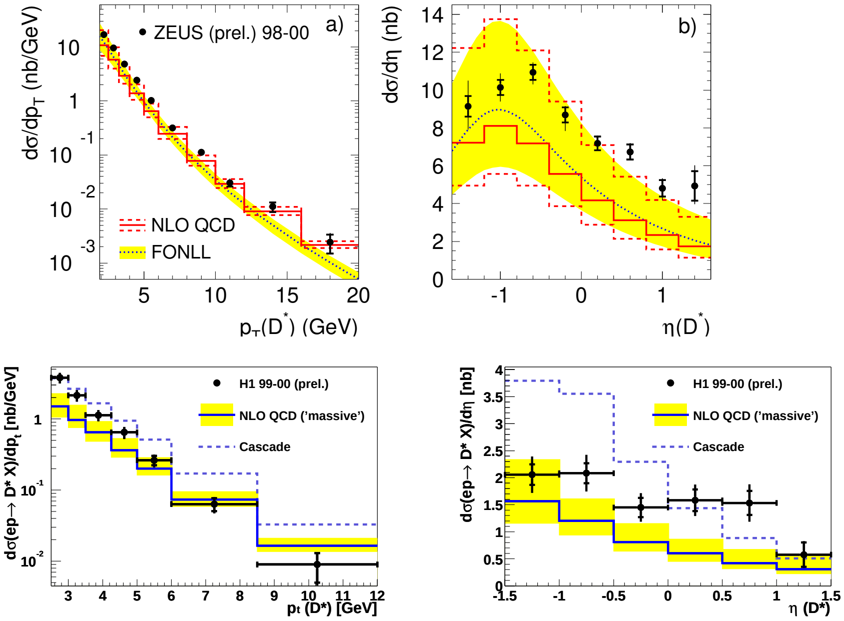

Figure 5: *Differential cross sections for inclusive $D^{*\pm}$ production in the process $ep \to D^{*\pm}X$. Top row: ZEUS The predictions of NLO calculations (+hadronisation corrections, solid histograms) and the FONLL predictions (dotted curves with shaded bands) are also shown. Bottom row: H1 with NLO (+hadronisation corrections, solid histogram and shaded region) and CASCADE (dashed histogram) predictions.*

measured [11] many parameters also in photoproduction, e.g. the fragmentation fractions of a charm quark to a particular charm hadron, $R_{u/d}$, γ_s and $V/(V+P)$. Cross section measurements of all D ground states, $D^{\pm}$, D^0, $D_S^{\pm}$ and also of $D^{*\pm}$ and Λ_c[4] were performed. Correcting for the small unmeasured amount of Ξ_c, a determination of the fragmentation fractions was possible just using data. Since some errors cancel in this way, the total errors are small and competitive with the world averages (dominated by e^+e^- measurements). The central values are in good agreement with previous H1 measurements in DIS [12].

The fragmentation function was determined by requiring a jet ($E_T > 9$ GeV, $|\eta^{jet}| < 2.4$) in addition to a $D^{*\pm}$ ($p_T^{D^*} > 2$ GeV^2, $|\eta^D| <$1.5). The resulting

[4] Kinematic region: $Q^2 < 1\,\mathrm{GeV}^2$; 130 $< W_{\gamma p} <$ 280 GeV; $p_T^{D,\Lambda} > 3.8$ GeV; $|\eta^{D,\Lambda}| <$1.6.

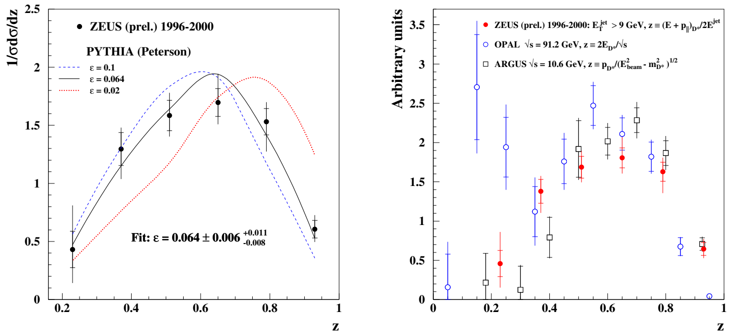

Figure 6: *Fragmentation measurement as a function of* $z = (E + p_{||})^D/(E + p_{||})_{\rm jet}$ *for the ZEUS data [11] and* $z = E_D/E_{\rm beam}$ *for the* e^+e^- *experiments OPAL and ARGUS.*

distributions of:

$$z = \frac{(E + P_{||})^{D^*}}{(E + P_{||})_{jet}} = \frac{(E + P_{||})^{D^*}}{2E_{jet}}$$

are shown in figures 6a and b. In figure 6a the data are compared with the one-parameter Peterson function. The parameter ϵ is determined to be $\epsilon = 0.064$, compatible with the value derived from the ARGUS data, $\epsilon \sim 0.053$. In figure 6b the universality of the fragmentation function is confirmed in comparison to ARGUS and OPAL data at $\sqrt{s} = 10.6$ GeV and 91.2 GeV, respectively.

4 Charmonium Production

Inelastic J/ψ production can be calculated within the framework of non–relativistic QCD (NRQCD) where the cross section is a sum over all possible intermediate $c\bar{c}$ states, including colour singlet (CS) and also colour octet (CO) states. The amplitude for each $c\bar{c}$ state with definite colour and angular momentum factorises into a short distance term which can be calculated in NRQCD and a long distance matrix element (LDME) describing the transition to a J/ψ. The LDME are not calculable and have been determined from J/ψ production data in $p\bar{p}$ collisions [14] where the CO contributions were found to be sizable. Charmonium production is measured in ep, $\gamma\, p$, $p\bar{p}$, $\gamma\gamma$ and in pA collisions. Previous HERA measurements show good agreement with the colour singlet term alone, which is the only term taken into account in the Colour Singlet Model (CSM), but small colour octet contributions could not be excluded.

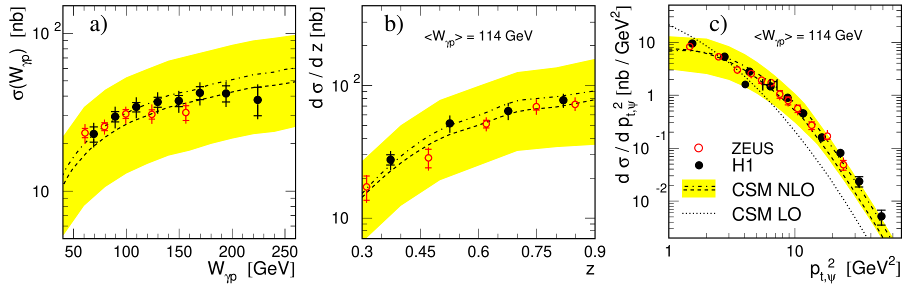

Figure 7: *a) Total J/ψ photoproduction cross section as a function of $W_{\gamma p}$ and differential cross sections as functions of b) $p^2_{t,\psi}$ and c) z. The ZEUS points [16] are shifted by up to 12% to account for differences in the covered kinematic range. The CSM calculations in NLO is shown by the band including normalization uncertainties due α_s and the charm mass.*

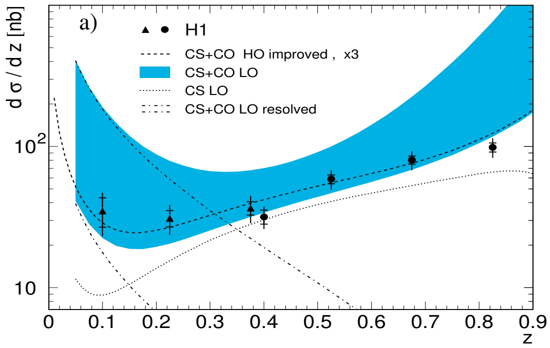

Figure 8: *Differential J/ψ photoproduction cross section ($120 < W_{\gamma p} < 260$ GeV) as a function of z in comparison to NRQCD calculations [18]. Note that contributions from b, χ_c or ψ', mainly contributing at low z are nor subtracted.*

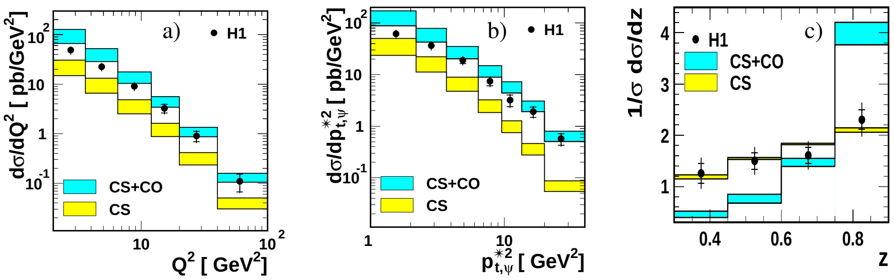

Figure 9: Differential J/ψ electroproduction cross section as a function of a) Q^2 and b) $p^{*2}_{t,\psi}$. c) Normalized differential cross section as a function of z. The data are compared to a full NRQCD calculation [19] (dark band) and to the LO colour singlet contribution alone (light band).

Recent results from H1 were obtained in photoproduction [15] in a large kinematic region. The cross sections for $0.3 < z < 0.9$ are shown in figure 7 in comparison with the ZEUS results [16]. Good agreement is found between the two experiments. The data are well described by a next–to leading order (NLO) calculation [17] in the Colour Singlet Model. In contrast, the LO calculation is much too steep in $p_{t,\psi}^2$. The elasticity distribution (Fig. 8 a) can also be described in the full range, $0.05 < z < 0.9$, by leading order NRQCD calculations [18] with LDMEs for the colour octet contributions at the lower end of the range allowed by the Tevatron data.

Inelastic electroproduction of J/ψ mesons [15] is studied in the region $2 < Q^2 < 100\,\mathrm{GeV}^2$ for medium elasticities $0.3 < z < 0.9$ and the squared transverse momentum of the J/ψ meson in the photon–proton center–of–mass system $p_{t,\psi}^{*2} > 1\,\mathrm{GeV}^2$. Neither the full NRQCD calculation [19] nor the colour singlet part can describe the data in normalisation (Fig. 9 a,b) over the full range. At high Q^2 and $p_{t,\psi}^{*2}$ agreement with the full NRQCD prediction is found. The dependence of the cross section on z, however, is well described by the CS contribution. The calculation including the CO contributions rises too strongly towards large z.

5 Beauty Production

Beauty Production at HERA is suppressed roughly by roughly two orders of magnitude compared to charm. Beauty events have mainly been detected through the decay of the b into leptons using the high average transverse momentum and/or lifetime information. The distribution of p_t^{rel}, the relative transverse momentum of the decay lepton with respect to the jet axis, which approximates the direction of the B-hadron in the case of b production, is used to fit the fraction of the b contribution.

H1 has in addition used the impact parameter of the decay lepton measured in the precise silicon vertex detector.

The first beauty measurements determined total cross sections [13] which showed an excess over the NLO pQCD calculations. Meanwhile, there are enough data to study differential distributions. A different strategy is pursued for this comparison: it is performed in the 'visible' kinematic region avoiding extrapolations. This however necessitates the implementation of hadronisation effects and heavy flavour decays in the NLO pQCD calculations.

The ZEUS collaboration presented differential cross sections in photoproduction selecting two jets with transverse energies of 7 and 6 GeV using the entire HERA I

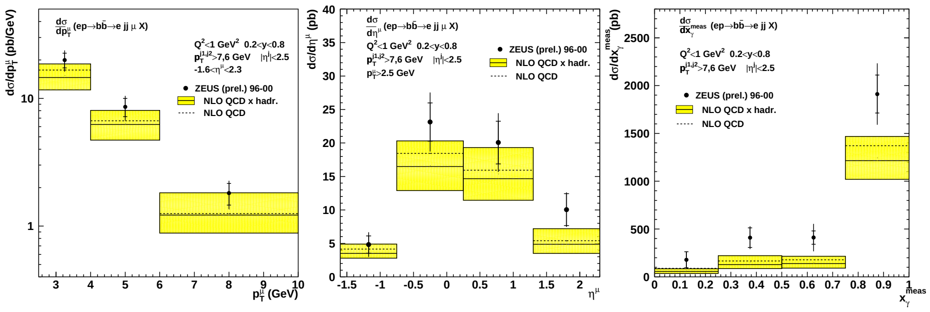

Figure 10: *Differential beauty cross sections as measured by ZEUS compared with NLO QCD calculations as a function of* p_t^μ, η^μ *and* x_γ^{obs} .

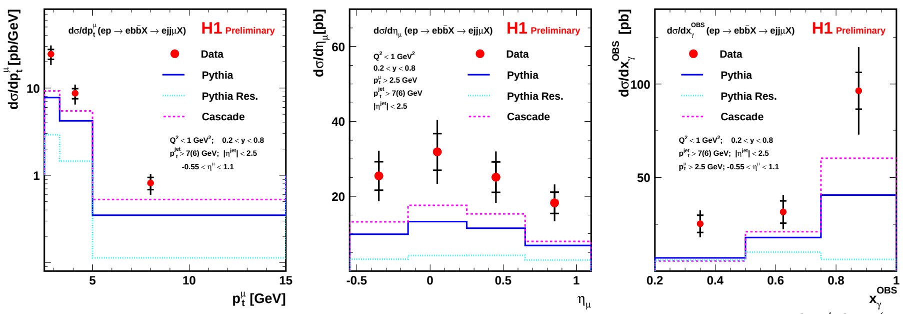

Figure 11: *Differential dijet muon beauty production cross section* $d\sigma/d\eta_\mu(ep \to eb\bar{b}X \to ejj\mu X)$ *as a function of* p_t^μ, η^μ *and* x_γ^{obs} *in the range* $Q^2 < 1$ GeV^2, $0.2 < y < 0.8$, $p_t^\mu > 2.5$ *GeV*, $-0.55 < \eta^\mu < 1.1$, $p_t^{jet_{1(2)}} > 7(6)$ *GeV and* $|\eta^{jet}| < 2.5$. *Also shown are the predictions of the Monte Carlo program PYTHIA (solid line), the resolved contribution to the PYTHIA cross section (dashed-dotted line) and the CASCADE prediction (dashed line).*

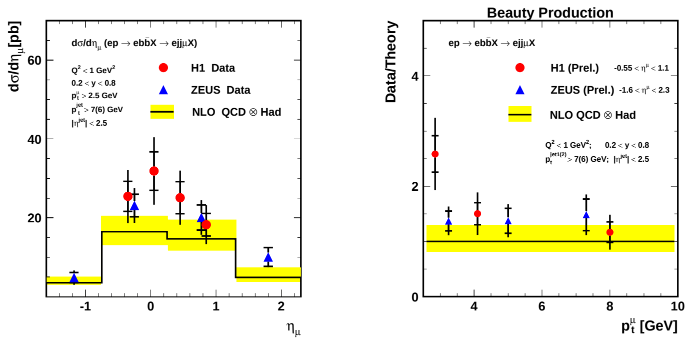

Figure 12: *Comparison of differential beauty cross sections as measured by H1 and ZEUS with NLO QCD calculations in photoproduction* ($Q^2 \sim 0$) *as a function of* η^μ *and* p_t^μ.

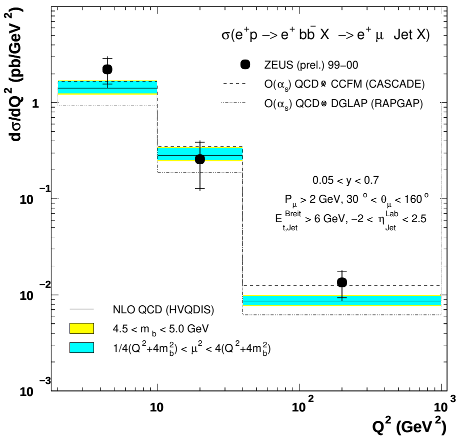

Figure 13: *Differential beauty cross section as a function of Q^2 for events with at least one jet reconstructed in the Breit frame and a muon, compared to the NLO QCD calculations. The shaded bands show the uncertainty of the theoretical prediction from the variation of the renormalisation and factorisation scales and the b-quark mass.*

data corresponding to 98 pb^{-1} [20]. The differential cross sections for the two jets and a μ in figures 10a and b are calculated in the visible region and show agreement of data and NLO calculation within errors (data/NLO $\sim$ 1.4). In figure 10c, x_γ^{obs}, the photon energy fraction in the 2 jet system, is shown after extrapolation of the muon into the unobserved phase space. Here, a factor 2 is observed between data and calculation. Very interesting is the observation of a b contribution at $x_\gamma^{obs} < 0.75$ which is expected to be dominated by resolved photon events.

A recent H1 analysis [21] selects photoproduction events with two jets and a muon, combining the p_t^{rel} and the impact parameter of the muon to determine the b fraction. Differential cross sections in the visible region of the two jets and the muon (jjμ) are shown in figures 11 and 12. The kinematic region covered is different from the ZEUS experiment, but agreement within errors is observed in the common region. The comparison with NLO QCD calculations including hadronisation yields agreement within 1.5 σ.

A ZEUS measurement of beauty at $Q^2 > 2$ GeV^2 is shown in figure 13 [22]. The data are compared with the NLO QCD calculations including hadronisation, which

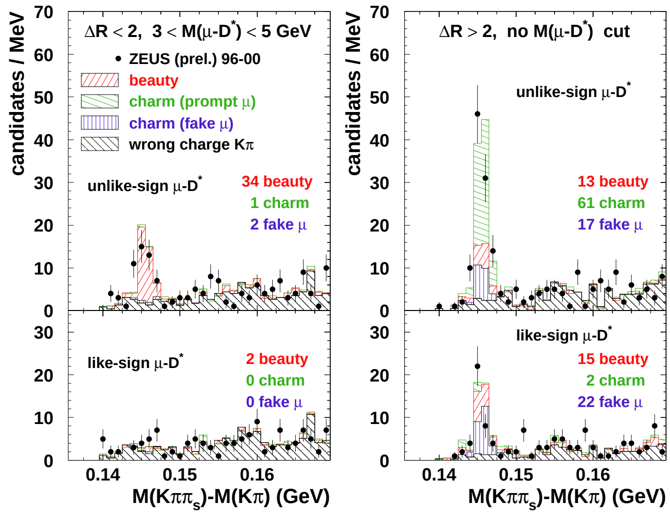

Figure 14: $\Delta M(D^* - D^0)$ *distributions for four different regions of phase space. The data are shown as full circles. The beauty and charm contributions, and the fake muon and combinatorial* D^* *backgrounds are indicated as shown in the legend. The rounded number of beauty, charm and fake-muon candidates is indicated in each figure.*

give a rather good description. A comparison with the Monte Carlo model CASCADE also shows good agreement while RAPGAP yields low results.

All recent data shown are preliminary, but one lesson is clear already: comparisons within the visible regions tend to give better agreement between data and NLO QCD calculations supplemented by hadronisation effects taken from the Monte Carlo models than previous comparisons which used extrapolations.

A new interesting analysis has been performed by both H1 [24] and ZEUS [23]. D^* and muons are reconstructed simultaneously leading to 'double tagged' events. The relative charge and opening angle can be used to enrich either charm pairs or beauty pairs. As an example, the ZEUS analysis is shown in figure 14. The top row shows unlike sign $D^* - \mu$ pairs with $\Delta R < 2$ (left) in which the beauty contribution dominates ($R = \sqrt{\Delta\eta^2 + \Delta\phi^2}$). This region can then be used to extract the beauty cross section. The result agrees with previous inclusive measurements within the limited statistics. In this selection the strong cuts on the transverse momentum of the D^*

and μ are not necessary, thus yielding access to an unexplored region of phase space.

Conclusion

New data on open charm and beauty production have been presented and discussed in comparison with other data and with theoretical predictions from pQCD. For charm production, systematic deviations between data and theory are observed in some kinematic regions. The agreement of data and theory tends to get better at higher Q^2. For beauty production, the comparison of differential cross sections in the experimentally visible region seems to give better agreement between data and NLO pQCD than previous total extrapolated cross sections. Although agreement of data and theory is roughly at the 1.5σ level, all data are above the calculations. Photoproduction of charmonium is well described by the colour singlet model in NLO. Small colour octet contributions can be accomodated in the data. The agreement of data and NRQCD calculations improves with increasing Q^2.

Acknowledgements

I thank the DIS'03 organisers for a fruitful meeting in impressive surroundings and my ZEUS and H1 colleagues for assistance in preparing the data and the talk.

References

[1] S. Frixione et al., Phys. Lett. B **348** (1995) 633 and Nucl. Phys. B **454** (1995) 3

[2] B.W.Harris and J.Smith, Phys. Rev. D**57** (1998) 2806

[3] M. Cacciari, S. Frixione and P. Nason, JHEP **0103** (2001) 006; [hep-ph/0102134]

[4] E.Norrbin and T.Sjostrand, Eur. Phys. J. C**17** (2000) 137; T. Sjostrand et al., Comput. Phys. Commun. **135** (2001) 238 [hep-ph/0010017]

[5] G. Marchesini et al., Comput. Phys. Commun. **67** (1992) 465

[6] H. Jung, Comput. Phys. Commun. **86** (1995) 147

[7] H. Jung and G.P. Salam, Eur. Phys. J. C **19** (2001) 351

[8] H1 Coll., Contr. paper H1-prelim-03-074

[9] H1 Coll., Contr. paper H1-prelim-03-071

[10] ZEUS Coll., Contr. paper 786 to ICHEP 2002, Amsterdam

[11] ZEUS Coll., Contr. paper 778 to ICHEP 2002, Amsterdam; contr. paper 564 to EPS 2003, Aachen

[12] H1 Coll., Contr. paper H1-prelim-02-076

[13] H1 Coll., C.Adloff et al, Phys.Lett. B 467, 156 (1999);
ZEUS Coll., J.Breitweg et al., Eur.Phys.J. C**18**, 625 (2001);
H1 Coll., Contr. paper 1013 to ICHEP 2002, Amsterdam

[14] F. Abe *et al.* [CDF Coll.], Phys. Rev. Lett. **79** (1997) 572.

[15] C. Adloff *et al.* [H1 Coll.], Eur. Phys. J. C**25** (2002) 1, 25-39.;
C. Adloff *et al.* [H1 Coll.], Eur. Phys. J. C**25** (2002) 1, 41

[16] S. Chekanov *et al.* [ZEUS Collaboration], arXiv:hep-ex/0211011

[17] M. Krämer, Nucl. Phys. B **459** (1996) 3

[18] M. Krämer, Prog. Part. Nucl. Phys. **47** (2001) 141 ;
B.A. Kniehl and G. Kramer, Eur. Phys. J. C **6** (1999) 493

[19] B.A. Kniehl and L. Zwirner, Nucl. Phys. B **621** (2000) 337

[20] ZEUS Coll., Contr. paper 785 to ICHEP 2002, Amsterdam

[21] H1 Coll., Contr. paper H1-prelim-03-072 to EPS 2003

[22] ZEUS Coll., Contr. paper 783 to ICHEP 2002, Amsterdam

[23] ZEUS Coll., Contr. paper 784 to ICHEP 2002

[24] H1 Coll., Contr. paper H1-prelim-02-071

The preliminary results can be found via http://www-h1.desy.de/h1/www/publications/conf/conf_list.html and http://www-zeus.desy.de/physics/hfla/public/PublicResults/ but see also contributions in these proceedings.